Design of chirped-coupling sidewall Bragg gratings for narrow linewidth distributed feedback lasers

EUGENIO DI GAETANO,[1,*] MARC SOREL[1]

[1]School of Engineering, University of Glasgow, Glasgow, United Kingdom
**Corresponding author: e.di-gaetano.1@research.gla.ac.uk*

Received XX Month XXXX; revised XX Month, XXXX; accepted XX Month XXXX; posted XX Month XXXX (Doc. ID XXXXX); published XX Month XXXX

A chirped-coupling sidewall Bragg grating is proposed to mitigate the nonlinear effects that deteriorate the linewidth in DFB lasers operating at a high power and current regime. This novel grating geometry is analyzed and simulated to extract the optimal design parameters in terms of intra-cavity field distribution. Compared to lasers with uniform Bragg gratings, devices fabricated with a chirped-coupling grating are shown to operate in stable single mode operation over a wider current and power range and exhibit linewidth as narrow as 100 kHz.

OCIS codes: (050.1590) Chirping; (050.2770) Grating; (140.3490) Lasers, distributed-feedback; (290.3700) Linewidth.

http://dx.doi.org/10.1364/OL.99.099999

A wide range of applications in telecommunications, sensing, metrology and quantum, such as laser cooling for atomic clocks, require high power, stable and narrow linewidth optical sources in the infrared spectral region. Amongst the various options, distributed feedback (DFB) semiconductor diode lasers are the ideal solution in all those scenarios that demand a compact device with high power efficiency and low fabrication costs. DFB operation in semiconductor lasers is achieved by defining a Bragg grating that induces a periodical modulation of the index or the gain along the lasing cavity [1]. To favour single mode operation, the Bragg grating design often includes a phase-shift quarter wavelength layer that is necessary to fulfil the second Barkhausen's condition of zero roundtrip phase shift [2]. However, the phase-shift layer also acts as a point defect in the periodical structure that increases the non-uniformity in the intra-cavity field distribution, which exacerbates the so called longitudinal spatial hole burning (LSHB) under high power operation [3]. This well-studied effect deteriorates the laser stability and increases the lasing linewidth [4]. Several grating designs were proposed in the past to mitigate LSHB, including higher-order gratings [5], distributed phase-shift layers [6,7] and chirped grating periods [8-11].

In this work we propose an alternative approach, used in the past for dispersion compensation in fiber Bragg gratings [12,13], which exploits the chirp of the grating coupling rather than the grating period. This solution is simple to implement in a semiconductor grating structure and, crucially, requires less strict fabrication accuracy and tolerances in comparison to previous methods.

The Bragg grating in our devices is made by etching a rectangular-shaped corrugation on the sidewalls of the optical waveguide, which defines two sections with different widths, i.e. w_1 and w_2, of the ridge waveguide to generate the required distributed modal refractive index contrast, (Fig. 1(a)). To ensure single mode transversal operation the range of values for the ridge waveguide widths w_1 and w_2 is between 2 µm and 3 µm. The grating coupling factor, or coupling per unit length, can be described by equation [14]:

$$\kappa = \frac{\left(n_2^{\,2} - n_1^{\,2}\right)}{n_{eff}\lambda_B m}\Gamma \sin\left(\pi m D\right) \tag{1}$$

where n_{eff} is the average modal effective index of the guided mode, n_2 and n_1 are the refractive indices of the materials forming the grating, λ_B is the wavelength satisfying the Bragg condition, m is the grating order, D is the grating duty cycle (i.e. the ratio between the lengths of the two ridge sections) and Γ is the optical modal confinement in the grating area. For simplicity, in the case considered here the structure is a first order grating, i.e. $m = 1$, with a 50% duty cycle, i.e. $D = \frac{1}{2}$. The average effective modal index n_{eff} and the modal confinement in the grating area Γ are extracted through a Finite Difference Eigenmode (FDE) 2D-simulation by Lumerical Mode solution [15] applying a longitudinal averaging of the transverse refractive index distribution [14]. An example of the simulated mode profile is given in Fig. 1(b).

The effective modal indices $n_{eff,1}$ and $n_{eff,2}$, extracted by 2D FDE simulations from the modal profile for the ridge waveguide with widths w_1 and w_2 provide the guided mode effective index $n(z)$ as a function of the longitudinal position along the cavity, i.e. the z-axis. From the $n(z)$ function, the electric field distribution along the cavity can be calculated by solving the time-independent propagation equation [1]:

$$\frac{d^2E}{dz^2} + \left[n(z)\frac{2\pi}{\lambda}\right]^2 E = 0 \tag{2}$$

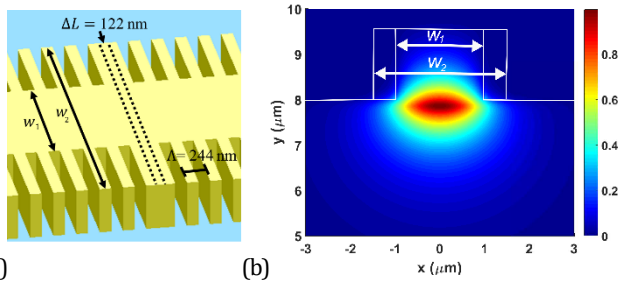

(a) (b)

Fig. 1. Schematic view of the sidewall grating geometry (a) and the simulation of the normalized electrical field for the transverse fundamental quasi-TE mode distribution in a ridge waveguide (b).

Eq. (2) can be decomposed in its left- and right-propagating components which combine together give the coupled mode equations [1]. The field distribution along the longitudinal z-axis was obtained through 1D FDE solver simulations since the analytical solution of the coupled mode equations is non-trivial for complex refractive index function $n(z)$.

As previously stated, a uniform DFB grating cannot operate in a single-mode regime, unless the cavity mirror losses are made asymmetrical [2]. However, the mirror losses in a semiconductor DFB laser critically depend on the facet cleave position relative to the grating making this method unreliable. An alternative and widely adopted solution consists in the addition of a layer $\Delta L = \lambda_B/4n_{eff}$, called phase-shift layer, in the center of the grating, which lifts the mode degeneracy at the Bragg wavelength [2]. However, the normalized field distributions for both uniform and phase-shifted gratings shown in Fig. 2 clearly indicate that the phase-shifted grating has a pronounced maximum occurring at the location of the phase-shift layer. Because the recombination rate depends on the carrier density, such a non-uniform field distribution along the cavity is transferred to the carrier density, the refractive index and to the Bragg condition. This results in a broadening of the linewidth, a decrease of the Side-Mode Suppression Ratio (SMSR) and, in general, a decrease in the laser stability which is exacerbated when the laser operates at high power regimes [3,4]. The obvious solution to mitigate this effect is to produce a field distribution approaching that of the uniform grating but still keeping a $\frac{\lambda}{4}$ – phase-shift along the cavity. One approach is to distribute the phase-shift layer along the cavity [6,7]; however, the very critical fabrication accuracy required by this geometry limits its applicability. As an example, distributing the phase-shift layer over a 400 μm-long cavity of a laser emitting at 1550 nm would require a change in the relative dimension of each Bragg element by less than 0.1 nm, which represents a major challenge even for the most advanced lithographic techniques. Another common solution is to chirp the grating period around the phase-shift layer [8-11] with the aim to balance the intra-cavity field by adding a region with a lower grating period around the phase-shift layer. This approach is effective in making the field distribution closer to the uniform grating case but the chirp modifies the Bragg condition and the fabrication accuracy does not allow for a fine chirp of the grating. Rather than chirping the Bragg period, the approach we propose exploits the chirp of the grating coupling factor. The sidewall grating is extremely beneficial here as it provides an additional degree of freedom to engineer the grating coupling by changing the profile of

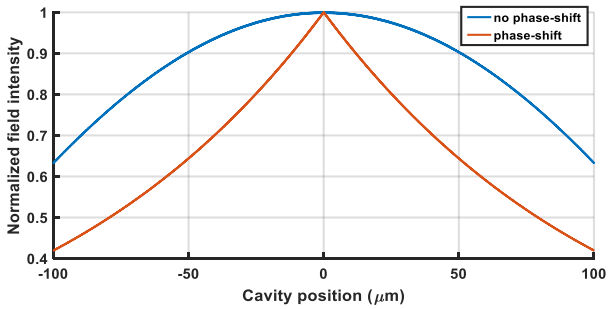

Fig. 2. Field distribution, normalized to the peak value, along the optical cavity for Bragg grating with and without the phase-shift layer. The cavity length is $L = 200$ μm with no reflectivity at the boundaries, and the grating coupling factor is $\kappa = 32$ cm^{-1}. Similar results in terms of field distribution profiles were obtained for different values of L and κ.

the corrugation in the transversal direction. A key advantage of this design is that the sensitivity of the effective mode index to changes in the transversal geometry is much lower than in the longitudinal geometry. In order to improve the field uniformity, the design strategy is to screen the effect of the phase-shift layer by creating a linear chirp of the coupling factor around the center of the grating (see Fig 3). The two parameters of interest for this design are the chirp length L_{chirp} and the coupling in the centre of the cavity κ_{min}. For large chirp lengths the screening effect is too much extended in the longitudinal dimension and generates an opposite field distribution (i.e. a lower field distribution in the center of the cavity and stronger close to the cavity facets).

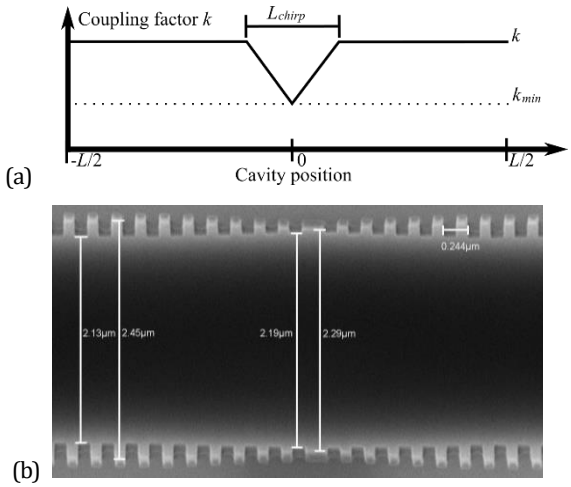

(a)

(b)

Fig. 3. Profile of the grating coupling along the optical cavity (a) and SEM picture of an example of its realization on a sidewall Bragg grating (b).

On the other hand, too small of a chirp length is difficult to implement and can create an abrupt field distribution. The simulations of the field distribution for different chirp lengths and a fixed coupling factor, i.e. κ_{min}=16 cm^{-1}, are shown in Fig. 4 (a). The difference in field distribution between chirped and uniform gratings, shown in Fig. 4 (b), indicates that 3 μm is the value of the chirp length that provides the closest field distribution to the uniform grating. Similar results were obtained for different values of the coupling factor κ_{min}. Simulations of the field distribution as a

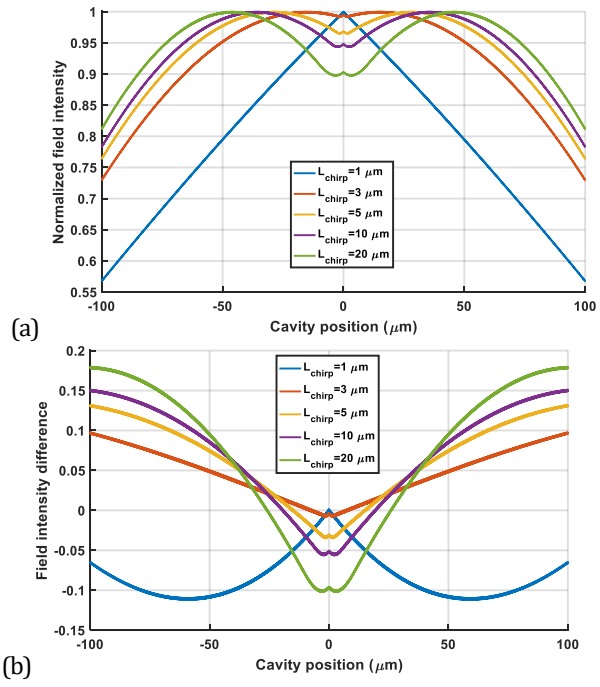

Fig. 4. Field distributions, normalized to the peak value, along the optical cavity for different chirp length L_{chirp} (a) and their difference with respect to no phase-shifted grating (b). The chirp amplitude is $\kappa_{min} = 16\ \mathrm{cm}^{-1}$ and coupling factor is $\kappa = 32\ \mathrm{cm}^{-1}$.

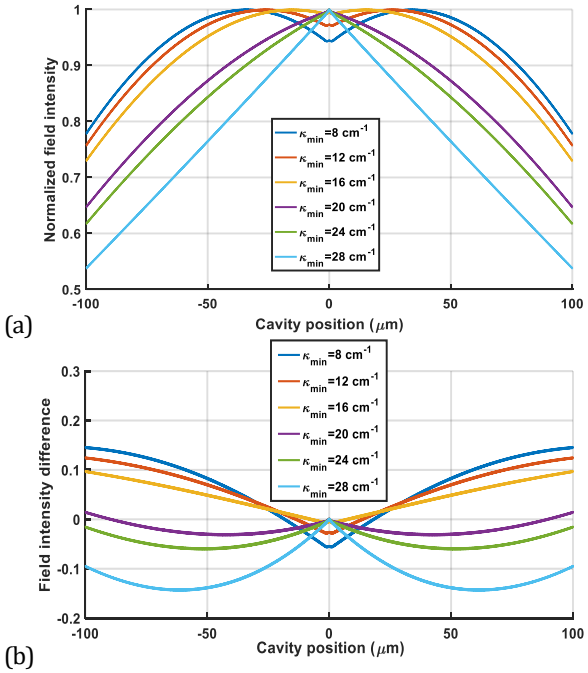

Fig. 5. Field distributions, normalized to the peak value, along the optical cavity for different coupling factors κ_{min} (a) and their difference with respect to no phase-shifted grating (b). The chirp length is $L_{chirp} = 3$ μm and coupling factor outside the chirped region is $\kappa = 32\ \mathrm{cm}^{-1}$.

function of the grating coupling in the centre of the cavity κ_{min} for a fixed chirp length of 3 μm are shown in Fig. 5 (a). The field distribution that best match the uniform case is obtained for $\kappa_{min} \approx 16 - 20\ \mathrm{cm}^{-1}$ (see figure 5(b)). As a general rule, the simulations show $L_{chirp} = 3$ μm and $\kappa_{min} \approx \kappa/2$ as optimal chirp parameters regardless of the cavity length L and coupling factor κ. This grating design offers two key advantages: i) the inclusion of the coupling-chirp does not modify the Bragg condition, ii) the fabrication accuracy and tolerances are substantially relaxed compared to previously reported designs. The former can be demonstrated by considering the effect of the variation of the ridge widths w_1 and w_2 on both the coupling factor and average modal index. The coupling factor κ value has a strong dependence on the difference between w_1 and w_2 whereas the average modal index n_{eff} is a function of the average between the effective indices $n_{eff,1}$ and $n_{eff,2}$: $n_{eff} \approx \sqrt{D\left(n_{eff,2}\right)^2 + (1-D)\left(n_{eff,1}\right)^2}$. Therefore, the ridge widths w_1 and w_2 can be optimized to obtain the desired coupling factor κ without modifying the average modal index n_{eff} as reported in previous works [16]. To prove the second point let us consider the coupling chirp optimal parameters $\kappa_{min} \approx 16\ \mathrm{cm}^{-1}$ and $L_{chirp} = 3$ μm previously calculated. The simulated values of κ show that the coupling-chirp requires a change in the transversal dimension between consecutive elements of the grating of 17 nm. Such value is over two orders of magnitude larger than the 0.1 nm dimensional change required for the phase-shift design distributed over a 400 μm-long cavity. Based on the simulation results, a sample including several device geometries was designed and fabricated. The swept device parameters were the cavity length L and coupling factor κ, as well as the chirp amplitude κ_{min}, whereas the chirp length $L_{chirp} = 3$ μm was kept constant. Due to the lack of available AR/HR coatings for this fabrication run, the devices were cleaved on one side only (i.e. R ~ 0.27), whereas the second facet had a tilted and down-tapered waveguide which couples the light into the substrate eliminating the end reflectivity (i.e. R ~ 0) in order to minimizes any Fabry-Perot cavity effects [16]. Both the chirped and un-chirped devices exhibited optical power values of approximately 20mW at a biasing current of 500mA. It is worth to note that because of the tilted and down-tapered waveguide used in these devices most of the optical power is dissipated into the substrate from the back of the cavity. AR/HR coated devices are expected to emit power levels 5 times larger. The devices with a field distribution closer to the uniform Bragg grating are expected to exhibit better stability for higher power and injected current. In particular, because the linewidth broadening at high current is a consequence of the LSHB, a reduction in the LSHB should lead to narrower emission linewidths, since the laser linewidth is proportional to the inverse of the power output $\Delta\nu \propto 1/\mathrm{P_{output}}$ as stated by the Schawlow-Townes formula [17].

The devices were fabricated on a 3QW AlGaInAs/InP material emitting at 1560 nm wavelength with a single-step shallow dry etch, described in previous works [18,19]. The laser linewidth characterization of the fabricated devices was measured through the heterodyne detection technique [20]. From the measured beat note signal, the linewidth is extrapolated from the fitting with a Voigt-shape profile, which is the typical lineshape expected from DFB semiconductor lasers. The measured linewidth as a function of the injection current is shown in Fig. 6 for two laser cavity lengths of $L = 2$ and 3 mm , for different coupling factors k_{min}, and fixed chirp length and coupling factor L_{chirp}= 3 μm and $\kappa = 32\ \mathrm{cm}^{-1}$, respectively. The uniform grating devices exhibit linewidth

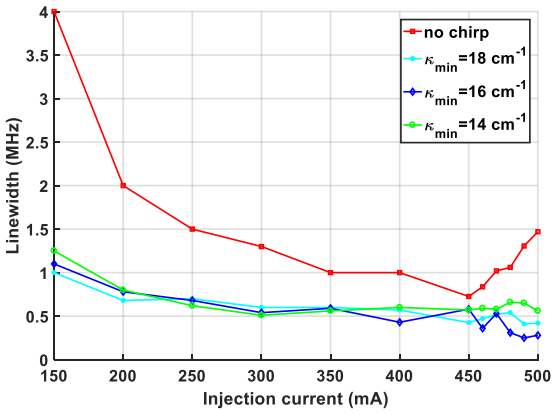

(a)

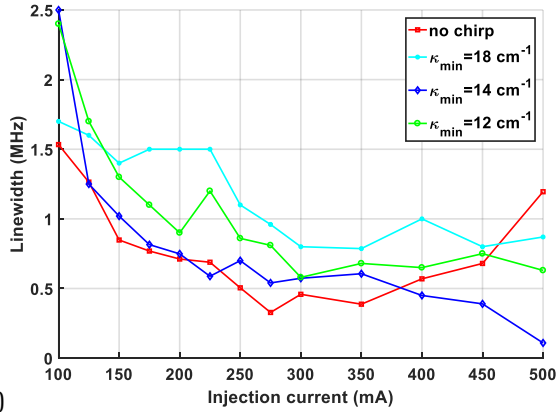

(b)

Fig. 6. Measured linewidth as a function of the injection current for 2 mm (a) and 3 mm (b) cavity lengths of the DFB laser with end reflectivities R ~ 0.27 and R ~ 0.

broadening at a current of approximately 450 mA and 350 mA for the 2-mm- and 3-mm-long cavities, respectively. By contrast, the chirped devices do not show any evident linewidth broadening within the current range considered here (i.e. 500 mA which is the upper limit of the current driver used). Among the chirped devices, the best performance in terms of quantum efficiency and linewidth were obtained for chirp amplitudes κ_{min} close to half of the grating coupling factor κ, thus, confirming the simulation of the field distribution, i.e. $\kappa_{min} \approx \kappa/2$. For the optimal design, the measured linewidth was as narrow as 109 kHz, as shown in Fig. 7, with potentially narrower linewidth values obtainable for injection current over 500 mA. In conclusion, a novel chirped-coupling Bragg grating design has been analyzed, simulated and fabricated in order to mitigate the detrimental effect of LSHB in phase-shifted DFB semiconductor lasers. The devices containing the chirped-coupling grating exhibit better performance with regards to linewidth broadening and absolute linewidth values than devices fabricated with a uniform grating. Moreover, the chirped-coupling grating design provides advantages in terms of wavelength insensitivity and substantially relaxed fabrication tolerances in comparison to other techniques, such as period chirps or distributed phase-shifts. It is worth pointing out that the design strategy we adopted here was to shape the coupling-chirp so as to match the longitudinal field profile of a uniform grating without a phase-shift. Because the flexibility of this approach allows to arbitrary shape the intra-cavity field, alternative design criteria can easily be explored to either further improve the lasing linewidth or increase the output power.

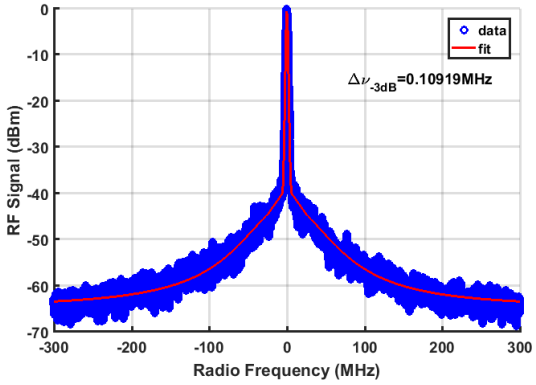

Fig. 7. RF beat note signal and Voigt fit for the narrowest achieved linewidth signal with FWHM of 109 kHz (single sweep, sweep time=6.7 ms, RBW=2.7 MHz, VBW=100 kHz).

Funding. Defence Science and Technology Laboratory (DSTL)

Acknowledgment. The authors would like to acknowledge the technical staff at the James Watt Nanofabrication Centre at Glasgow University and Vincenzo Pusino for valuable discussions.

References

1. H. Kogelnik and C. V. Shank, J. Appl. Phys., **43,** 2327 (1972)
2. J. Buus, IEEE Proceedings, Part J, **133,** 163 (1986)
3. H. Soda, Y. Kotaki, H. Sudo, H. Ishikawa, S . Yamakoshi and H. Imai, J . Quantum Electron., **QE-23**, 804 (1987).
4. H. J. Wünsche, U. Bandelow and H. Wenzel, J . Quantum Electron., **29**, 1751 (1993)
5. A. Akrout, K. Dridi and T. J. Hall, *Photonics North* (SPIE, 2012), Vol. 8412
6. G. P. Agrawal, J. E. Geusic and P.J. Anthony, Appl. Phys. Lett. **53,** 178 (1988)
7. M. Okai, M. Suzuki, T. Taniwatari, Elec. Lett. **29,** 1696 (1993)
8. P. Zhou and G. S. Lee, Appl. Phys. Lett. **56,** 1400 (1990)
9. P. Zhou and G. S. Lee, Elec. Lett. **26**, 1660 (1990)
10. P. Zhou and G. S. Lee, Appl. Phys. Lett. **58,** 331 (1991)
11. P. Zhou and G. S. Lee, J. Appl. Phys. **70,** 1902 (1991)
12. M. J. Strain and M. Sorel, Photon. Tech. Lett. **18,** 2566 (2006)
13. M. J. Strain and M. Sorel, Photon. Tech. Lett. **20**, 1863 (2008)
14. T. Uusitalo, H. Virtanen and M. Dumitrescu, Opt. Quant. Electron., **49**, 206 (2017)
15. http://www.lumerical .com/mode.php
16. M. Zanola, M. J. Strain, G. Giuliani and M. Sorel, Photon. Tech. Lett., **24**, 1063 (2012)
17. C. H. Henry ,J . Quantum Electron., **19**, 1391 (1983)
18. L. Hou, M. Haji, J. Akbar, B. Qiu and A. C. Bryce, Opt. Lett., **36,** 966 (2011)
19. L. Hou, M. Haji, J. Akbar and J. H. Marsh, Opt. Lett., **37**, 4525 (2012)
20. S. Spiessberger, M. Schiemangk, A. Wicht, H. Wenzel, O. Brox and G. Erbert, J. Lightw. Tech. **18**, 2611 (2010)

Full References

1. H. Kogelnik and C. V. Shank, "Coupled-Wave Theory of Distributed Feedback Lasers" Journal of Appled Physics., Vol. 43, No. 5, pp. 2327-2335 (1972)
2. J. Buus, "Dynamic single-mode operation of DFB lasers with phase shifted gratings and reflecting mirrors" IEEE Proceedings J - Optoelectronics, Vol. 133, No. 2 pp. 163-164 (1986)
3. H. Soda, Y. Kotaki, H. Sudo, H. Ishikawa, S . Yamakoshi and H. Imai, "Stability in single longitudinal mode operation in GaInAsP/InP phase-adjusted DFB lasers", Journal of Quantum Electronics., Vol. 23, No. 6, pp. 804-814 (1987).
4. H. J. Wünsche, U. Bandelow and H. Wenzel, "Calculation of combined lateral and longitudinal spatial hole burning in lambda/4 DFB lasers" Journal of Quantum Electronics, Vol. 29, No. 6, pp. 1751-1760 (1993)
5. A. Akrout, K. Dridi and T. J. Hall, "Investigation of longitudinal spatial-hole burning in high-order laterally coupled distributed feedback lasers", *Photonics North*, Proceedings SPIE, Vol. 8412, No. 841219 (2012)
6. G. P. Agrawal, J. E. Geusic and P. J. Anthony, "Distributed feedback lasers with multiple phase-shift regions", Applied Physics Letters, Vol. 53, No. 3, pp. 178-179, 1988
7. M. Okai, M. Suzuki, T. Taniwatari, "Strained multiquantum-well corrugation-pitch-modulated distributed feedback laser with ultranarrow (3.6kHz) spectral linewidth", Eletronics Letters, Vol. 29, No. 19, pp. 1696-1697, 1993
8. P. Zhou and G. S. Lee, "Mode selection and spatial hole burning suppression of a chirped grating distributed feedback laser", Applied Physics Letters, vol. 56, no. 15, pp. 1400-1402, 1990
9. P. Zhou and G. S. Lee, "Chirped grating lambda/4-shifted distributed feedback laser with uniform longitudinal field distribution" Electronics Letters, Vol. 26, No. 20, pp.1660-1661 (1990)
10. P. Zhou and G. S. Lee, "Phase-shifted distributed feedback laser with linearly chirped grating for narrow linewidth and high-power operation", Applied Physics Letters, Vol. 58, No. 4, pp. 331-333 (1991)
11. P. Zhou and G. S. Lee, "Mechanism of phase-shifted distributed-feedback laser with linearly chirped grating for stable-mode operation", vol. 70, no. 3, pp. 1902-1904, 1991
12. M. J. Strain and M. Sorel, "Post-Growth Fabrication and Characterization of Integrated Chirped Bragg Gratings on GaAs-AlGaAs", Photonics Technology Letters, Vol. 18, No. 24, pp. 2566-2568 (2006)
13. M. J. Strain and M. Sorel, "Integrated III-V Bragg Gratings for Arbitrary Control Over Chirp and Coupling Coefficient" Photonics Technology Letters, Vol. 20, No. 22, pp. 1863-1865 (2008)
14. T. Uusitalo, H. Virtanen and M. Dumitrescu, "Transverse structure optimization of distributed feedback and distributed Bragg reflector lasers with surface gratings," Optical and Quantum Electronics, Vol. 49, No. 6, pp. 206-216 (2017)
15. http://www.lumerical .com/mode.php
16. M. Zanola, M. J. Strain, G. Giuliani and M. Sorel, "Post-Growth Fabrication of Multiple Wavelength DFB Laser Arrays With Precise Wavelength Spacing", Photonics Technology Letters, Vol. 24, No. 12, pp. 1063-1065 (2012)
17. C. H. Henry, "Theory of the phase noise and power spectrum of a single mode injection laser", Journal of Quantum Electronics, Vol. 19, No. 9, pp. 1391-1397 (1983)
18. L. Hou, M. Haji, J. Akbar, B. Qiu and A. C. Bryce, "Low divergence angle and low jitter 40 GHz AlGaInAs/InP 1.55um mode-locked lasers", Optics Letters, Vol. 36, No. 6, pp. 966-968 (2011)
19. L. Hou, M. Haji, J. Akbar and J. H. Marsh, "Narrow linewidth laterally coupled 1.55 μm AlGaInAs/InP distributed feedback lasers integrated with a curved tapered semiconductor optical amplifier", Optics Letters, Vol. 37, No. 21, pp. 4525-4527 (2012)
20. S. Spiessberger, M. Schiemangk, A. Wicht, H. Wenzel, O. Brox and G. Erbert, "Narrow Linewidth DFB Lasers Emitting Near a Wavelength of 1064 nm" Journal of Lightwave Technology, Vol. 18, No. 17, pp. 2611-2616 (2010)